The performance of guardrail is related closely to soil. Calcote and Kimball (1978) carried out pendulum tests on two guardrail posts installed in five different soil types and found that guardrail installations less than the recommended minimum length failed with severe impacts when installed in the poorer soils. Numerical methods are employed to study the interaction between the guardrail post and soil (Rohde et al. 1996; Plaxico et al. 1998; Wu and Thomson 2007). Rohde et al. (1996) demonstrated the differences in the failure mechanisms of post between stiff and soft cohesive soils and noncohesive soils by both stress distributions and total stresses measured with the pressure transducers.

In this paper, the miniature cone penetration test (MCPT) is used to characterize the post subsoil strength, and the experimental relation of the lateral bearing capacity of the guardrail post with the limit cone tip resistance of subsoil in MCPT is obtained. The model of soil reaction distribution on the post was presented and the reaction distribution coefficient in the model was obtained based on MCPT. According to the model, the reinforcement method of the post in weak subsoil was put forward.

MINIATURE CONE PENETRATION TESTS OF SUBSOIL

Subsoil for test was silty clay and was from the subgrade of the 4th Ring Road of Beijing. Water content of soil ranged from 9.85% to 13.85%. In order to obtain different strength of soil for tests, the compaction degrees were controlled from 79.1% to 97.7%. Before each loading test of post, MCPTs were performed to characterize the strength of soil. The Miniature cone penetrometer used is shown in Fig.2. Fig.3 shows the shape of the cone. In MCPTs, four kinds of cones were used. Though their maximum diameter were all 14mm, they had different cone angle, 19.85°, 22.62°, 26.03° and 31.28°, respectively. The diameter of the cone shaft was 7.3mm. Because cone shaft diameter is less than the diameter of cone, the frictional resistance of cone shaft was ignored and only the cone tip resistance was considered as the cone penetration resistance.

The cone tip resistance tends to be stable when attending to a critical depth, as shown in Fig.4. The stable cone tip resistance herein is called as limit cone tip resistance q_{cl}. It was also found that the cone tip resistance has no correlation with the cone angle. In test, the limit cone tip resistance q_{cl} is the average value from different cone angles.

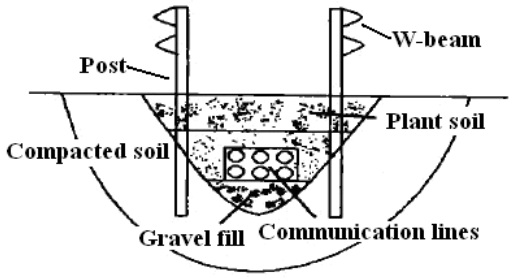

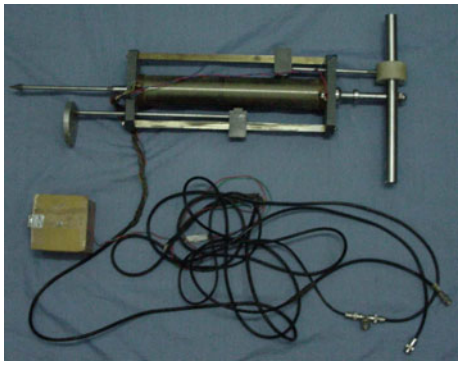

Fig.1. Diagram of central separate belt. **Fig. 2. Miniature cone penetiometer.**

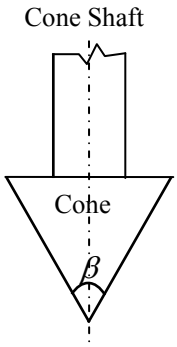

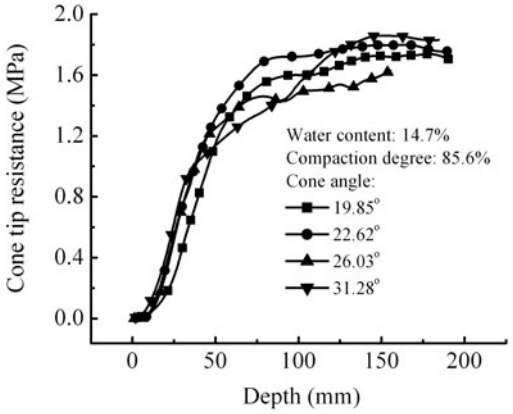

Fig. 3. Shape of the cone. **Fig. 4 Curves of penetration resistance vs. depth.**

LATERAL LOADING TESTS OF GUARDRAIL POSTS

In tests, the post was embedded in a test chamber. The chamber is 1.73m in width, 1.86m in length and 1.25m in depth. The diameter of the post is 114mm and the wall thickness is 4mm, respectively. The embedding depth of the post is 1.2m. The height of loading point on post is 0.6m, the same as the height of W-beam shown in Fig.1. In each test, only one post was loaded, as shown in Fig.5.

Fig.6 shows the curves of the lateral load vs. the horizontal displacement of loading point. The limit cone tip resistances of subsoil corresponding to the curve No.1, No.2 and No.3 in Fig.6 were 1.17MPa, 2.03MPa and 2.27MPa, respectively. The behavior of the post under lateral load depends on the strength of subsoil. When the soil is soft, the post is not bent and behaves as the rigid pile, as the curve No.1. When the soil is harder, the local buckling of the post happens and the lateral load descends sharply when the horizontal displacement attends a certain value. Under the impacting load of the vehicle out of control, the post is bent to absorb energy. The bent posts behave as curves No.2 and No.3. From curves No.2, No.3 and other curves of bent posts, some laws can be seen:

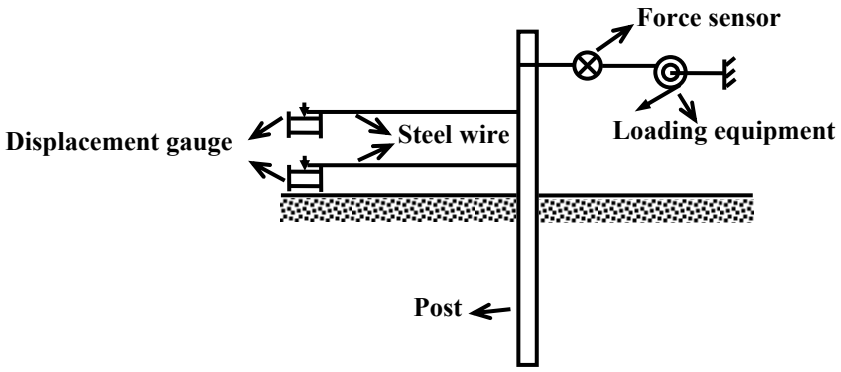

Fig. 5. Layout diagram of test equipments of post.

(1) The initial segment of the load-displacement curve is straight line. However, with the increase of the displacement, the lateral load increases nonlinearly, and then the second straight line segment appears on the curve. Once the local buckling happens, the lateral load will decrease sharply.
(2) The load at the intersection point of the extension lines of two straight line segments on the load-displacement curve is called as critical load P_{cr}. When the lateral load is less than P_{cr}, the subsoil around the post is linear elastic. The maximum load on the curve is called as buckling load P_b. P_{cr} and P_b both increase with the increase of the strength of soil. After carrying out a series of loading tests of posts, the following equations were obtained:

$$P_{cr} = 0.0038\, q_{cl} \quad (1)$$

$$P_b = 0.0092\, q_{cl} \quad (2)$$

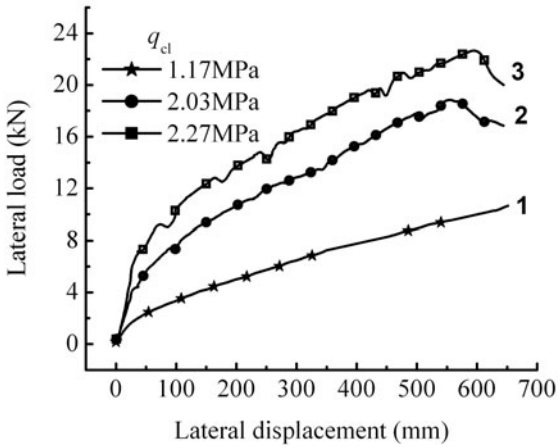

Fig. 6. Curve of load vs. displacement of loading point.

MODEL OF SOIL REACTION DISTRIBUTION ON POST

In order to guarantee the safety margin of the post, the critical load P_{cr} is taken as the allowable load. From Eq. 1 an Eq. 2, it can be seen that P_b is 2.42 times of P_{cr}, so the safety factor of post is 2.42.

Based on the MCPTs, assuming the soil reaction on post is in direct proportion to the limit cone tip resistance, a model of soil reaction distribution is presented corresponding to P_{cr}, as shown in Fig. 7. In Fig. 7, B and l are the diameter and the embedding depth of post, respectively; h is the height of the loading point on the post; f is the depth of the maximum moment point on the post; H is the distance of rotation center from the bottom of the post; α is the coefficient of the soil reaction and dimensionless. Before the buckling failure of post, the post rotates around the rotation center point that moves along the post with the increase of the loading. In Fig. 7, above the rotation center point, the right side and left side of post are subject to the passive and active soil pressure, respectively. However, this is contrary under the rotation center point. Herein assume that the total soil pressure at any point of post is not related to the depth. According to loading tests of posts, the coefficient of the soil reaction α was obtained by back calculation.

(1) At the maximum bending moment point on the post, the shear force is zero, so

$$-p_{cr}+\alpha q_{cl}Bf=0 \tag{3}$$

$$f=\frac{p_{cr}}{\alpha q_{cl}B} \tag{4}$$

(2) According to the equilibrium of the lateral forces on the post, the following equations can be obtained:

$$P_{cr}-\alpha q_{cl}Bl+2\alpha BHq_{cl}=0 \tag{5}$$

$$H=\frac{\alpha q_{cl}Bl-P_{cr}}{2\alpha Bq_{cl}}=\frac{1}{2}(l-f) \tag{6}$$

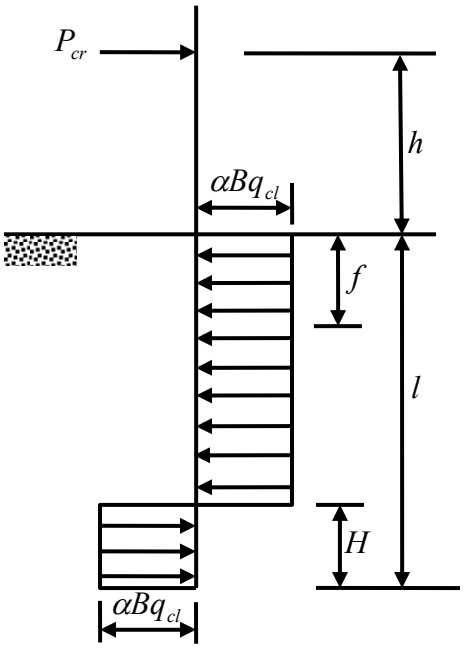

Fig. 7. Model of soil reaction distribution on post.

(3) According to the equilibrium of the force moment, the following equations can be obtained:

$$p_{cr}(l+h)-\frac{\alpha q_{cl}Bl^2}{2}+\alpha q_{cl}BH^2=0 \tag{7}$$

From Eq.4, Eq.6 and Eq.7, we can obtain

$$p_{cr}=\alpha B^2 q_{cl}\left\{\sqrt{\left[\left(\frac{l}{B}\right)+2\left(\frac{h}{B}\right)\right]^2+\left(\frac{l}{B}\right)^2}-\left[\left(\frac{l}{B}\right)+2\left(\frac{h}{B}\right)\right]\right\} \tag{8}$$

For the post, l = 1.2m, h = 0.6m, B = 0.114m, so

$$p_{cr}=0.0323\alpha q_{cl} \tag{9}$$

From Eq.1 and Eq.9, we can obtain α = 0.118. According to Eq. 4 and Eq. 6, f = 0.283m, H = 0.458m. By comparison, it is found that the difference of the measured and calculated results is less than 5% for f and 1% for H.

REINFORCEMENT METHOD OF POST

In order to reinforce the post, a rectangular steel plate was vertically inserted to subsoil, touching closely with the post side opposite to the lane. The plate has an included angle of 15° with the lane direction, as shown in Fig.8. The thickness of the plate is 10mm and the height t is taken as 0.618 times of the width b according to golden section rule. The anticorrosion requirement of the plate is the same as the post.

In the central separate belt of the expressway, the subsoil is different. The upper is the plant soil and the lower is the compacted soil, as shown in Fig.1. The limit cone tip resistances of the upper and the lower subsoil are expressed with q_{cl1} and q_{cl2}, respectively. Similar with the model shown in Fig.7, the soil reaction is assumed to be in direct proportion to the limit cone tip resistance and the effective width of post. In the range of the plate height under ground, the effective width of the post is the width of the plate, however, elsewhere is the diameter of the post. The proportional coefficient of soil reaction α is invariable and equal to 0.118. The model of soil reaction distribution on the reinforced post is as shown in Fig.9.

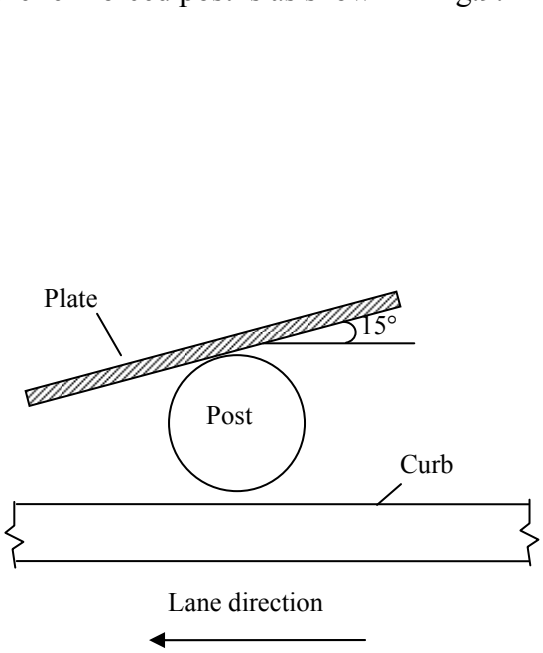

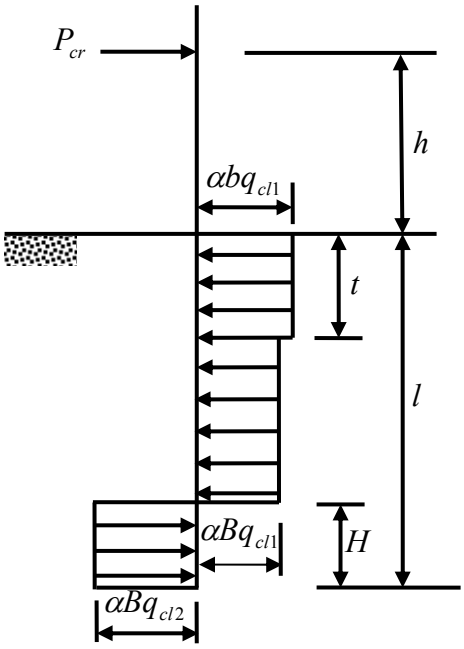

Fig. 8. Planeform of reinforced post. **Fig. 9. Soil reaction distribution model of reinforced post.**

For compacted soil in the roadbed, the design compaction degree is 96% and the moisture content is optimum in China. For the silty clay used in tests, the limit cone tip resistance of the compacted silty clay is 2.27MPa and the corresponding critical load of post embedding totally in the compacted soil is 8656.2N according to Eq. 1. So in the Fig.9, q_{cl2} = 2.27MPa and the object of reinforcement of the post embedding partly in the plant soil is that the critical load attends to 8656.2N and is equivalent to the case of $q_{cl1} = q_{cl2} = 2.27$MPa.

According to the model shown in Fig.9, the dimension of steel plate corresponding to different strength of plant soil can be determined.

(1) According to the equilibrium of the lateral forces on the post, we obtain

$$P_{cr} - \alpha q_{cl1} Bl + \alpha BH(q_{cl1} + q_{cl2}) - \alpha q_{cl1}(b - B)t = 0 \quad (10)$$

$$H = \frac{\alpha q_{cl1} Bl + \alpha q_{cl1}(b - B)t - P_{cr}}{\alpha B(q_{cl1} + q_{cl2})} \quad (11)$$

(2) According to the equilibrium of the force moment, the following equations can be obtained:

$$p_{cr}(l + h) - \frac{\alpha q_{cl1} Bl^2}{2} + \frac{\alpha B(q_{cl1} + q_{cl2})H^2}{2} - \frac{\alpha q_{cl1}(b - B)(2l - t)t}{2} = 0 \quad (12)$$

From Eq.11 and Eq.12 , the relation between q_{cl1} and the dimension of the plate is obtained

$$q_{cl1} = \frac{-\Delta_2 - \sqrt{\Delta_2^2 - 4\Delta_1\Delta_3}}{2\Delta_1} \quad (13)$$

Where:

$\Delta_1 = \alpha^2 b(b - B)t^2$;

$\Delta_2 = 2\alpha BHp_{cr} - (\alpha Bl)^2 q_{cl2} - 2\alpha(b - B)tp_{cr} - \alpha^2 B(b - B)(2l - t)tq_{cl2}$;

and $\Delta_3 = 2\alpha B(l + h)p_{cr}q_{cl2} + p_{cr}^2$.

In Eq.13, $t = 0.618b$, $\alpha = 0.118$, $q_{cl2} = 2.27$ MPa, $p_{cr} = 8656.2$ N, $B = 0.114$ m, $h = 0.6$ m, $l = 1.2$ m. The relation of the width of the plate with the limit cone tip resistance of the plant soil is shown in Fig.10.

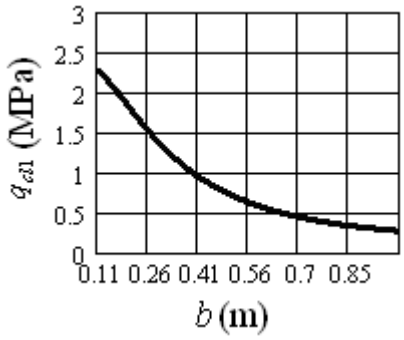

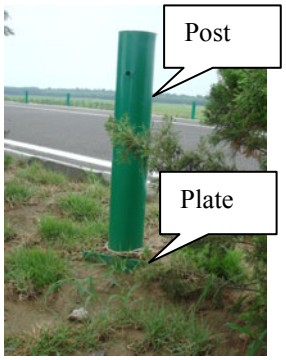

Fig. 10. Curve of q_{cl1} with b. **Fig. 11. Picture of reinforced post.**

VERIFICATION OF REINFORCEMENT METHOD OF POST

In order to verify the reinforcement method, a laterally loading test of post was carried out. In test, the upper subsoil is the plant soil, with the thickness of 0.75m and q_{cl1} = 1.3MPa. The lower subsoil is the compacted soil, with the thickness of 0.45m and q_{cl2} = 2.24MPa ≈ 2.27MPa. The dimension of the plate is from Fig.10, $b = 310$ mm and $t = 192$ mm. In verification test, the critical load of 9500N was obtained, more than the design load of 8656.2N. It is implied that the reinforcement method can satisfy the engineering requirement.

Now this reinforcement method has been applied to guardrail posts of some expressways of China, e.g., Rongwu expressway, as shown in Fig.11.

CONCLUSIONS

Laterally loading tests of the guardrail post in the central separate belt of the expressway were carriedout. The subsoil around the post is silty clay. In order to reflect the strength of subsoil, the parallel MCPTs were performed. In MCPT, when the penetration depth of cone attends a critical depth, the cone tip resistance tends to a limit resistance. For the post embedding totally in the compacted soil, there are two characteristic loads – the critical load and the buckling load. The critical load reflects the elastic or plastic state of soil and the buckling load reflects the anti-buckling capacity of the post. The critical load and buckling load are all related directly to the cone limit penetration resistance. Based on the limit cone tip resistance, a model of soil reaction distribution on the post embedding totally in the compacted soil was presented. The coefficient of the soil reaction was obtained by back calculation.

A steel-plate reinforcement method of the post embedding partly in plant soil was put forward. Based on the model of soil reaction distribution, the dimension of the reinforcing plate was determined. The reinforcement method was verified and found to satisfy the requirement of bearing capacity of the post.

ACKNOWLEDGMENTS

This work was supported by the Chinese Natural Science Foundations (Nos.51078222, 50708056 and 50978207), Shandong Province Reward Foundation for Excellent Young and Middle-aged Scientists(No.2008BS09015) and Independent Innovation Foundation of Shandong University, IIFSDU(No.2010JQ001).

REFERENCES

Calcote, L. R. and Kimball, C. E. (1978). "Properties of guardrail posts for various soil types." *Transportation Research Record*, No.679: 22-25.

Plaxico, C. A., Patzner, G. S. and Ray, M. H. (1998). "Finite-element modeling of guardrail timber posts and the post-soil interaction" *Transportation Research Record*, No.1647: 139-146.

Rohde, J. R., Rosson, B.T. and Smith, R. (1996). "Instrumentation for determination of guardrail-soil interaction." *Transportation Research Record*, No.1528: 109-115.

Wu, W. J. and Thomson, R. (2007). " Finite-element modeling of guardrail timber posts and the post-soil interaction." *International Journal of Impact Engineering*, Vol. 34(5): 883-898.

Wright, A. E., Ray, M. H. (1996). "Characterizing guardrail steel for LS-DYNA3D simulations." *Transportation Research Record*, No.1528: 138-145.

Study on the Ultimate Aseismic Capacity of High Core Rock-Fill Dam

Li Hongjun[1], Zhong Hong[2] and Chi Shichun[3]

[1]Senior Engineer, China Institute of Water Resources and Hydropower Research,, West Chegongzhuang Rd., Beijing 100044, China; **lijunli1995@163.com**.
[2] Lecturer, Faculty of Infrastructure Engineering, Dalian University of Technology, Dalian,People's Republic of China. hzhong@dlut.edu.cn.
[3] Professor, Faculty of Infrastructure Engineering, Dalian University of Technology, Dalian,People's Republic of China. schchi@dlut.edu.cn.

ABSTRACT: Since the "5.12" WenChuan Earthquake occurred in China, evaluation of the ultimate aseismic capacity has been a crucial issue for seismic safety design of high core rock-fill dams. However, reasonable evaluation of the ultimate aseismic capacity of high rock-fill dams still confuses the hydraulic engineers. Thus an original approach to evaluate the ultimate aseismic capacity is proposed. In this approach, the ultimate peak acceleration of input motion which the dam could tolerate is taken as an important index to evaluate the ultimate aseismic capacity. The ultimate peak acceleration can be directly achieved on the basis of 'Specifications for seismic design of hydraulic structures' instead of trial and error method. Then, the proposed method is adopted to evaluate the ultimate aseismic capacity of the 240m ChangHe high rock-fill dam. In addition, comprehensive studies on the dynamic response and potential failure mode as the rock-fill dam subjected to the ultimate tolerable input motion, that is, the rock-fill dam is at verge of failure, are presented. Consequently, the corresponding reinforced design for the high rock-fill dams can be carried out effectively on the basis of the dynamic analysis as the dam reach the ultimate limit equilibrium state.

INTRODUCTION

Since the "5.12" WenChuan Earthquake occurred in China, the safety of dams subjected to strong earthquake has draw more attention than ever. In order to enforce the aseismic work for the super high and important dams, the China Institute of Water Resources and Hydropower Research promulgates the NO.24 laws on the basis of the regulations issued by National Energy Administration. Rigorous study on the ultimate aseismic capacity of dams located seismic active zones, whose failure may result in serious secondary disasters must be performed. However, there has not been a reasonable method and criterion for the evaluation of ultimate aseismic capacity of high dams. Nowadays, many researchers have been aware of the crucial importance of this issue and devoted to relevant study. Zhao et. al (2009) used the trial and error method to study the ultimate aseismic capacity of rock-fill dams and conducted a

comprehensive analysis for the LiangHeKou high rock-fill dam on the dynamic stability of dam slope, the earthquake induced permanent deformation, the potential liquefaction of impervious core and filtering layer. He finally came to the conclusion that the ultimate aseismic capacity depended mainly on the safety of dam slopes. Li et. al (2010) studied the ultimate aseismic capacity of a high core rock-fill dam based on the dynamic responses for several input motions which have different peak accelerations. It is shown that the engineers can give reasonable reinforced measures based on the characteristics of dynamic response of dam as the dam reaches the ultimate limit equilibrium state. Based on the aforementioned research, we can find that the amplitude of peak acceleration can be taken as a reasonable index or criterion to evaluate the ultimate aseismic capacity of high rock-fill dams. In this paper, the ultimate peak acceleration which makes the factor of safety of dam slope equals to the design criterion (Fs = 1.20) regulated by the "Specifications for seismic design of hydraulic structures" (DL5073-2000 in China) can be determined accurately and directly by the pseudo-static method. In addition, reasonable aseismic measures can be performed based on the studies of sliding deformation and seismic safety of impervious body as the dam reaches its ultimate aseismic capacity.

Ultimate Aseismic Capacity *VS* Peak Acceleration

In traditional deterministic seismic slope stability analyses, the pseudo-static factor of safety is usually taken as an important criterion to evaluate the aseismic capacity of dam.

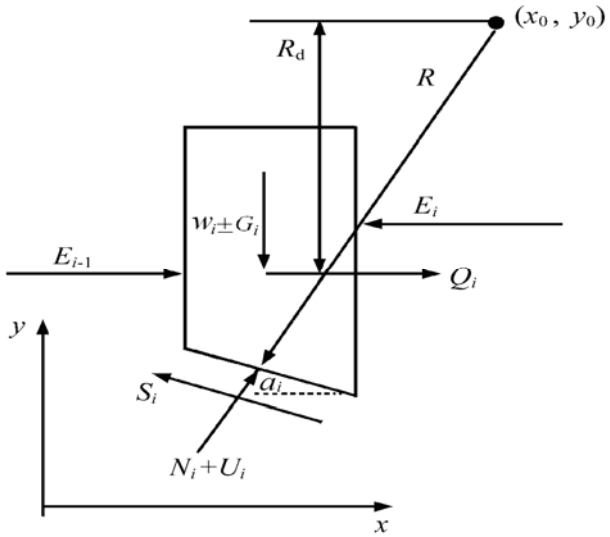

FIG. 1 Vector diagram of forces for the slice in pseudo-static method

With respect to Fig. 1, the original formulation by Bishop (1955) can be rewritten by taking into consideration the horizontal and vertical induced inertial forces. By solving simultaneously Eqs. (1), (2) and (3), the coefficient of peak acceleration a_{max} can be achieved directly for different tolerable standard of factor of safety.

$$F_S = \frac{\sum_{i=1}^{n} \frac{1.0}{m_{\alpha_i}} \times \left(((W_i \pm G_i) - u_i l_i \cos\alpha_i) \times \tan\phi_i' + c_i l_i \times \cos\alpha_i \right)}{\sum_{i=1}^{n} \left((W_i \pm G_i) \sin\alpha_i + Q_i \times \frac{R_d{}^i}{R} \right)} \quad (1)$$

$$m_{\alpha_i} = \cos\alpha_i + \frac{\tan\phi_i'}{F_s} \times \sin\alpha_i \quad (2)$$

$$Q_i = a_{\max} c_z a_i W_i \qquad G_i = W_i a_{vi} / g \quad (3)$$

$$a_{\max} = \frac{\frac{1}{Fs} \sum_{i=1}^{n} \frac{1.0}{m_{\alpha_i}} \times \left(((W_i \pm G_i) - u_i l_i \cos\alpha_i) \tan\phi_i' + c_i l_i \cos\alpha_i \right)}{\sum_{i=1}^{n} W_i a_i c_z \frac{R_d{}^i}{R}} - \frac{\sum_{i=1}^{n} (W_i \pm G_i) \sin\alpha_i}{\sum_{i=1}^{n} W_i a_i c_z \frac{R_d{}^i}{R}} \quad (4)$$

where, *F*s is factor of safety; c, ϕ' is cohesion and friction angle respectively; W is slice weight, u is pore-pressure; Q is horizontal inertial force of slice; G is vertical inertial force of slice, "positive" symbols downward; "negative" symbols upward; l is the length of slice bottom; α is the angle that the tangential line through the mid point with the horizontal; C_z is reduction factor in horizontal inertial force; a is the distribution coefficient of inertial force at slice centroid; a_{max} is coefficient of the peak acceleration of input motion; R_d is the vertical distance between the center and the centroid of slice.

According to 'Specifications for seismic design of hydraulic structures' (2000), the minimum tolerable factor of safety for the class one rock-fill dam subjected to strong earthquake is 1.2. Thus, the coefficient of peak acceleration which can make the factor of safety of the dam slope equal 1.2, can be determined by Eq. (4). The coefficient of peak acceleration for the ChangHe dam is about 0.52g. Consequently, it can be taken as the ultimate peak acceleration which the high rock-fill dam could bear, that is, the dam reaches the ultimate aseismic capacity. However, in order to achieve the reasonable reinforced measures which can prevent the occurrence of dam-break as the dam subjected to unexpected strong earthquake, the time-history of dynamic analysis for the dam with the ultimate peak acceleration should be carried out.

Dynamic Response of the ChangHe Dam Under the Limit Input Motion

The ChangHe dam, a clay core rock-fill dam is to be constructed in southwestern China. Its crest is 16m wide and 240m high, the upstream and downstream slopes are both at 2:1. Figure 2 shows the maximum cross section of the dam. The dam is mainly composed of core, filter, shell, and transitional material.